The Plant Cell, Vol. 20: 3389–3404, December 2008, www.plantcell.org

Calcium-Dependent Freezing Tolerance in *Arabidopsis* Involves Membrane Resealing via Synaptotagmin SYT1 [W]

Tomokazu Yamazaki,[a] Yukio Kawamura,[a,1] Anzu Minami,[a] and Matsuo Uemura[a,b]

[a] The 21st Century Center of Excellence Program, Iwate University, Morioka, Iwate 020-8550, Japan
[b] Cryobiofrontier Research Center, Faculty of Agriculture, Iwate University, Morioka, Iwate 020-8550, Japan

Plant freezing tolerance involves the prevention of lethal freeze-induced damage to the plasma membrane. We hypothesized that plant freezing tolerance involves membrane resealing, which, in animal cells, is accomplished by calcium-dependent exocytosis following mechanical disruption of the plasma membrane. In *Arabidopsis thaliana* protoplasts, extracellular calcium enhanced not only freezing tolerance but also tolerance to electroporation, which typically punctures the plasma membrane. However, calcium did not enhance survival when protoplasts were exposed to osmotic stress that mimicked freeze-induced dehydration. Calcium-dependent freezing tolerance was also detected with leaf sections in which ice crystals intruded into tissues. Interestingly, calcium-dependent freezing tolerance was inhibited by extracellular addition of an antibody against the cytosolic region of SYT1, a homolog of synaptotagmin known to be a calcium sensor that initiates exocytosis. This inhibition indicates that the puncture allowing the antibody to flow into the cytoplasm occurs during freeze/thawing. Thus, we propose that calcium-dependent freezing tolerance results from resealing of the punctured site. Protoplasts or leaf sections isolated from *Arabidopsis SYT1*-RNA interference (RNAi) plants lost calcium-dependent freezing tolerance, and intact *SYT1*-RNAi plants had lower freezing tolerance than control plants. Taken together, these findings suggest that calcium-dependent freezing tolerance results from membrane resealing and that this mechanism involves SYT1 function.

INTRODUCTION

Freezing tolerance is an important trait in plants living in areas with subzero temperatures in winter (Levitt, 1980). Because freezing results in multiple stresses (dehydration, mechanical and low temperature stress) to plant cells, it is difficult to understand exactly how plants live under freezing conditions. Many physiological and electron microscopy studies have indicated that irreversible damage first occurs at the plasma membrane when the temperature decreases below that which plants can tolerate (Levitt, 1980; Steponkus et al., 1993). Cold acclimation, which enhances the freezing tolerance of plants, minimizes the occurrence of freeze-induced plasma membrane lesions (Steponkus et al., 1993). Thus, it is reasonable to predict that the extent of freezing tolerance depends on the ability of plants to prevent damage to the plasma membrane.

The lipid composition of the plasma membrane is associated with differences in freezing tolerance among plant species and with the cold acclimation–induced increase in freezing tolerance (Uemura and Yoshida, 1984, 1986; Yoshida and Uemura, 1984; Lynch and Steponkus, 1987; Steponkus et al., 1993; Uemura and Steponkus, 1994). These differences and changes in lipid composition affect membrane cryobehavior, which accounts for some, but not all, of the freezing tolerance observed (Steponkus et al., 1993). On the other hand, many studies have demonstrated that gene expression and/or protein profiles, including those of plasma membrane proteins, change during cold acclimation (Uemura and Yoshida, 1984, 1986; Yoshida and Uemura, 1984; Yoshida, 1984; Thomashow, 1999; Seki et al., 2002a; Kawamura and Uemura, 2003; Los and Murata, 2004). Some proteins, such as dehydrins and lipocalin, may help prevent damage to the plasma membrane during freezing (Puhakainen et al., 2004; Uemura et al., 2006). These studies are based on the idea that plant cells avoid freeze-induced damage at the plasma membrane by changing the physicochemical characteristics of their membranes or by using hydrophilic substances.

In animal cells, even after the plasma membrane is damaged, cells can rapidly reseal damaged sites in the plasma membrane before they become lethal. This process is strictly dependent on extracellular calcium (Steinhardt et al., 1994). The plasma membrane is normally damaged in many animal cells that live in environments where mechanical forces arise as a result of physical activity, for example, in mammalian skeletal and cardiac muscle cells (for review, see McNeil and Kirchhausen, 2005). For membrane resealing, it is essential that some exocytotic event or vesicle–vesicle fusion starts as calcium flows from the extracellular space into the cytoplasm through the damaged sites. Two membrane resealing models have been proposed (McNeil and Kirchhausen, 2005). One is the facilitated resealing model, in which the decrease in membrane tension caused by extracellular calcium-dependent exocytosis can facilitate the self-resealing capacity of the membrane at the disrupted site. Another is the patching model, which explains the resealing mechanism when cells experience much larger membrane disruption. In this model, after the calcium influx triggers vesicle–vesicle fusion,

[1] Address correspondence to ykawa@iwate-u.ac.jp.
The author responsible for distribution of materials integral to the findings presented in this article in accordance with the policy described in the Instructions for Authors (www.plantcell.org) is: Yukio Kawamura (ykawa@iwate-u.ac.jp).
[W] Online version contains Web-only data.
www.plantcell.org/cgi/doi/10.1105/tpc.108.062679

large patch vesicles are formed and finally fused to the plasma membrane in an exocytotic manner.

Generally, it is recognized that plasma membrane resealing in animal cells is a biologically complex and tightly regulated process (McNeil and Kirchhausen, 2005). Membrane resealing involves many kinds of proteins, including soluble *N*-ethylmaleimide-sensitive factor attachment protein receptor (SNARE) proteins, synaptotagmin VII, annexin A1, dysferlin, and calpain (Steinhardt et al., 1994; Bi et al., 1995; Reddy et al., 2001; Bansal et al., 2003; Chakrabarti et al., 2003; Shen et al., 2005; McNeil et al., 2006; Mellgren et al., 2007). The interaction between SNARE proteins and synaptotagmin is essential for calcium-triggered membrane–membrane fusion during exocytosis (for review, see Jackson and Chapman, 2006; Lynch et al., 2007). Mammalian synaptotagmins form a gene family in which a transmembrane domain at the N terminus and two tandem calcium binding domains (C_2A and C_2B domains) at the C terminus are conserved (Craxton, 2004). Because synaptotagmin is a calcium sensor during exocytosis, synaptotagmin VII has been proposed to start the membrane resealing process induced by calcium influx (Reddy et al., 2001).

During a freeze/thaw cycle, plant cells are considered to receive mechanical stress induced by freeze-induced dehydration, thaw-induced rehydration, and ice crystal growth (Levitt, 1980), although it is unknown whether the plasma membrane is mechanically punctured during freeze/thawing. Interestingly, it has been observed that microvesicles in the vicinity of the plasma membrane cause vesicle–vesicle fusion and/or exocytotic events under freezing conditions (Fujikawa and Takabe, 1996; Yamazaki et al., 2008). In addition, we found that the levels of a plasma membrane protein, SYT1 (At2g20990), an *Arabidopsis thaliana* synaptotagmin homolog that was previously called *AtSytA* (Craxton, 2004), increased rapidly in parallel with the acquisition of freezing tolerance during cold acclimation (Kawamura and Uemura, 2003). Considering these findings, we tested a working hypothesis that plant cells actively protect the plasma membrane during the freeze/thawing process using a system similar to membrane resealing in animal cells.

Herein, we show the calcium dependency of freezing tolerance at the cell and tissue levels. In some cases, we added a specific antibody against the cytosolic C_2A domain of SYT1 in the suspension buffer. On the basis of physiological and immunohistochemical results, we concluded that the tolerance of cells to mechanical stress associated with ice crystal growth depends considerably on the presence of extracellular calcium, which is related to membrane resealing. We also show not only that *SYT1*-RNAi (for RNA interference) or T-DNA insertion mutants lose this calcium-dependent freezing tolerance, but also that their freezing tolerance is decreased at the whole-plant level. Thus, SYT1-associated membrane resealing at the cellular level affects the freezing tolerance of whole plants.

RESULTS

Extracellular Calcium-Dependent Freezing Tolerance of Protoplasts

Because extracellular calcium is essential for membrane resealing in animal cells (Steinhardt et al., 1994), we first determined the survival of protoplasts isolated from *Arabidopsis* leaves that were nonacclimated or cold-acclimated for 1 or 7 d (AC1d or AC7d) following a freeze/thaw cycle in the presence (1 mM $CaCl_2$) or absence (1 mM EGTA) of calcium. Although cold acclimation resulted in an increase in survival in the presence of either calcium or EGTA, survival in the presence of calcium was much higher than that in the presence of EGTA (Figure 1A). These results indicate that both nonacclimated and cold-acclimated cells possess calcium-dependent freezing tolerance. Calcium-dependent survival, which is defined as the difference between survival in the presence of calcium and that in the presence of EGTA, increased during the course of cold acclimation (Figure 1B). In nonacclimated protoplasts, calcium-dependent survival was a maximum of ~30% at –2°C, but decreased as the temperature lowered. In cold-acclimated protoplasts, however, calcium-dependent survival was kept at ~30 to 40% at temperatures ranging from –2 to –10°C (AC1d) or from –2 to –14°C (AC7d). Thus, the freezing tolerance of protoplasts was substantially dependent on extracellular calcium in the suspending medium; furthermore, cold acclimation remarkably enhanced calcium-dependent freezing tolerance.

To further investigate the effect of extracellular calcium during a freeze/thaw cycle, survival of protoplasts isolated from AC7d leaves was measured after freezing to –8°C in the presence of various concentrations of calcium (0 to 10 mM) (Figure 2A). Survival of protoplasts frozen at 0 or 0.1 mM calcium was only slightly higher than that in the presence of EGTA, but the difference was not statistically significant. Survival began to increase

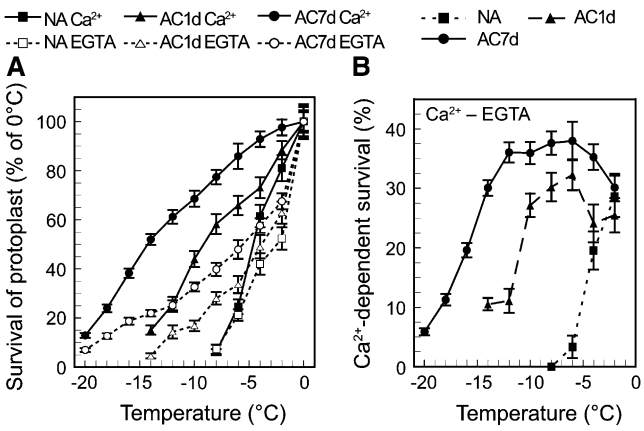

Figure 1. Extracellular Calcium-Dependent Freezing Tolerance of Protoplasts.

(A) Freezing tolerance was determined in protoplasts isolated from leaves that were nonacclimated (NA; square) or cold-acclimated for 1 d (AC1d; triangle) or 7 d (AC7d; circle) in the presence of 1 mM $CaCl_2$ (closed) or 1 mM EGTA (open). After freezing, cell survival was measured by fluorescein diacetate staining. Survival of unfrozen protoplasts that were kept at 0°C was taken as 100%. Data are means ± SE (n = 9).

(B) Calcium-dependent survival was calculated as the difference between the survival in the presence of calcium and that in the presence of EGTA. Data are shown for protoplasts isolated from *Arabidopsis* leaves that were nonacclimated (NA; closed square) or cold-acclimated for 1 d (AC1d; closed triangle) or 7 d (AC7d; closed circle).

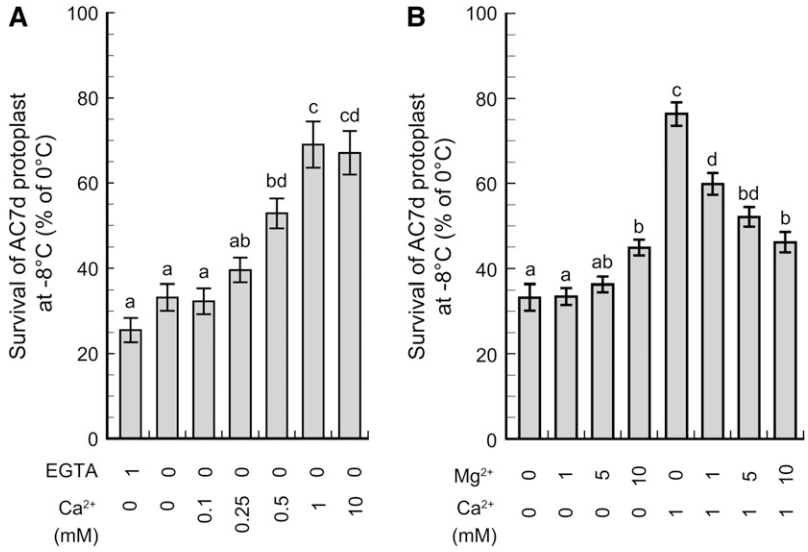

Figure 2. Effect of Calcium and Magnesium Concentrations on Calcium-Dependent Freezing Tolerance.

(A) Using protoplasts isolated from AC7d leaves, survival was measured after freezing to –8°C. The concentrations of EGTA and calcium are indicated at the bottom of the panel. Data are means ± SE (n = 6 to 11).

(B) Using protoplasts isolated from AC7d leaves, survival was measured after freezing to –8°C. The concentrations of magnesium and calcium are indicated at the bottom of the panel. When neither magnesium nor calcium was added, 1 mM EGTA was added to chelate the two cations completely. Data are means ± SE (n = 6 to 12). Different letters indicate statistically significant differences between treatments by one-way analysis of variance (ANOVA) with Tukey-Kramer multiple comparison test ($P < 0.05$).

significantly at 0.25 mM calcium and reached a maximum at 1 mM. Because calcium-dependent membrane resealing is competitively inhibited by magnesium (Steinhardt et al., 1994), we next focused on the effect of magnesium on freezing tolerance. Interestingly, the freezing tolerance that was enhanced by 1 mM calcium almost disappeared when 10 mM magnesium was added, suggesting that magnesium may be able to bind the site where calcium functions to enhance freezing tolerance (Figure 2B).

To reveal the process by which calcium increases freeze/thaw survival, two experiments were performed using protoplasts isolated from AC7d leaves. First, the effect of calcium during freezing was tested. Protoplasts were frozen in the presence of 1 mM calcium, and then an excess amount of EGTA was added just before thawing began to chelate calcium ions from the melting solution surrounding protoplasts (final concentration of 0.5 mM calcium and 5 mM EGTA after the suspension medium was completely melted). However, this addition of EGTA during thawing did not affect calcium-dependent freezing tolerance (cf. lanes 2 and 3 in Figure 3A). On the other hand, because the survival of protoplasts frozen in the presence of 0.5 mM calcium and 5 mM EGTA was almost the same as that in the presence of 5 mM EGTA (cf. lanes 1 and 4 in Figure 3A), there was effectively no calcium present during thawing in the experiment illustrated in lane 3 in Figure 3A, suggesting that calcium affects survival during freezing. Second, to test the effect of calcium during thawing, protoplasts were frozen in the absence of calcium, but calcium was added into the sample just before thawing began (a final concentration of 1 mM calcium after thawing). Even in this case, calcium-dependent freezing tolerance was observed (Figure 3B). Thus, these two results suggest that calcium-dependent freezing tolerance requires calcium during either freezing or thawing.

During a freeze/thaw cycle, the plasma membranes of protoplasts may suffer mechanical stresses primarily as a result of three causes: (1) freeze-induced dehydration, (2) thaw-induced rehydration, and (3) pressure by ice crystal growth. Freeze-induced dehydration and thaw-induced rehydration have been simulated by exposing protoplasts to a hypertonic solution and then returning them into an isotonic solution (Steponkus et al., 1993). Ice at –4°C is calculated to cause dehydration equivalent to the extent when subjected to ~2.15 osmol solutions (Towill and Mazur, 1976). According to this calculation, protoplasts from an isotonic solution (0.6 M sorbitol) were first exposed to a hypertonic solution containing 2.15 M sorbitol to simulate the mechanical stress caused by freeze-induced dehydration and then placed back under an isotonic condition by the addition of appropriate volume of no-sorbitol solution to mimic thaw-induced rehydration. Survival of protoplasts in the presence of 1 mM $CaCl_2$ was similar to that in the presence of 1 mM EGTA (Figure 4A). Next, to study the effect of direct mechanical stress on the plant plasma membrane, such that caused by ice crystal growth, the survival of protoplasts was measured after electroporation in the presence of 1 mM $CaCl_2$ or 1 mM EGTA. Interestingly, survival after electroporation in the presence of calcium was significantly higher than that in the presence of EGTA (Figure 4A) (Student's t test, $P < 0.05$). These results collectively suggest that the calcium-dependent freezing tolerance of protoplasts is due to the mitigation of mechanical stresses on the plasma membrane imposed by ice crystal growth, but not imposed by freeze-induced dehydration and/or thaw-induced rehydration.

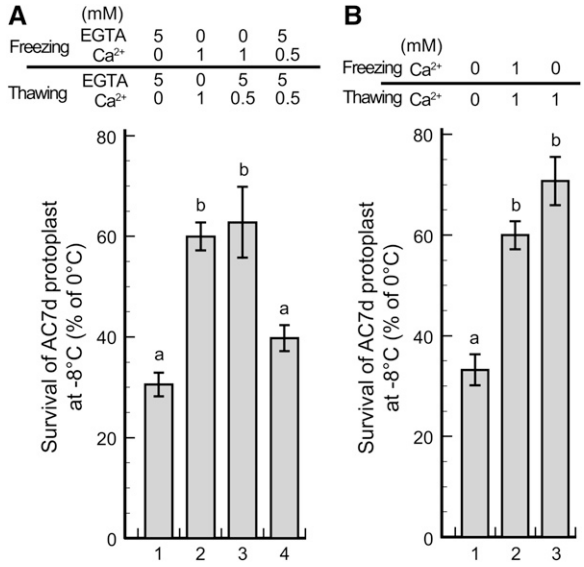

Figure 3. Effect of Calcium during the Freezing and Thawing Processes.

(A) The effect of calcium during freezing was tested. Using protoplasts isolated from AC7d leaves, survival was measured after freeze/thawing to –8°C in the presence of 5 mM EGTA (lane 1), 1 mM $CaCl_2$ (lane 2), or 0.5 mM $CaCl_2$ and 5 mM EGTA (lane 4). In another test, after being frozen in the presence of 1 mM calcium, an equal aliquot of the suspension solution containing 10 mM EGTA was added just before thawing began (final concentrations of 0.5 mM calcium and 5 mM EGTA after thawing) (lane 3). Data are means ± SE (n = 4).

(B) The effect of calcium during thawing was tested. Using protoplasts isolated from AC7d leaves, survival was measured after freeze/thawing to –8°C in the presence of 0 mM (lane 1) or 1 mM $CaCl_2$ (lane 2). In another test, after protoplasts were frozen in the absence of calcium, an equal aliquot of the suspension solution including 2 mM calcium was added just before thawing began (to a final concentration of 1 mM calcium after thawing) (lane 3). Data are means ± SE (n = 4). Different letters indicate statistically significant differences between treatments by one-way ANOVA with Tukey-Kramer multiple comparison test ($P < 0.05$).

Calcium-Dependent Freezing Tolerance of Leaf Sections

Although protoplasts have often been used in studies of plant freezing tolerance because of the advantages in controlling the environment around the cells, the protoplast system cannot evaluate the influence of cell walls. Thus, we next studied calcium-dependent freezing tolerance in thin leaf sections (70 to 80 μm in thickness) prepared from AC7d leaves using the cryomicroscope. When leaf sections were immersed and frozen in a solution without sorbitol, survival was significantly higher in the presence of 1 mM calcium than in the presence of 1 mM EGTA or 0 mM calcium (Figure 5A), which is similar to the results with protoplasts (Figure 1A). Interestingly, survival in the presence of 0 mM calcium was somewhat higher than that in the presence of EGTA (Figure 5A), as we will discuss later. When leaf sections were immersed in 0.6 M sorbitol, however, there were no differences in survival in the presence or absence of extracellular calcium (Figure 5B). Thus, the calcium-dependent freezing tolerance was only detected when leaf sections were immersed in a solution with no osmoticum. Interestingly, the results shown in Figure 5 further revealed that the freezing tolerance of *Arabidopsis* leaf sections is considerably dependent on the osmolarity of the solution around leaf sections: in the presence of 1 mM calcium, survival of cells in leaf sections immersed in a solution without sorbitol was ~56% at –3°C (Figure 5A), but much greater (~70%) even at –12°C when immersed in a solution containing 0.6 M sorbitol (Figure 5B). This is consistent with the results of Murai and Yoshida (1998), who showed that the freezing tolerance of Jerusalem artichoke tuber tissues is remarkably lower in water than in an isotonic solution.

During cryomicroscopic observation, we noticed that ice distribution in tissues seems to be different when the tissues are immersed and frozen in the presence or absence of 0.6 M sorbitol. This difference may be associated with the unfrozen volume of the solution in these two experiments. According to a calculation by Towill and Mazur (1976), the unfrozen volume is much less in the solution without sorbitol (0.2% at −3°C) than in a solution containing 0.6 M sorbitol (9% at −12°C). To explore the possibility that ice distribution in the tissue influences the survival of cells, the ice distribution in leaf sections was observed after

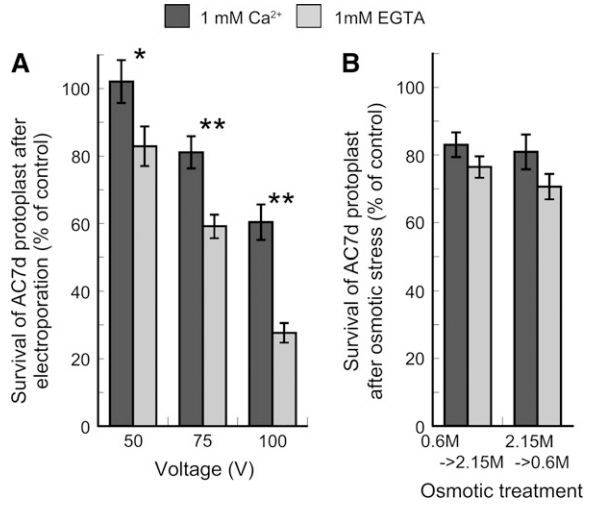

Figure 4. Effect of Calcium on Tolerance to Mechanical or Osmotic Stress.

(A) Protoplasts isolated from AC7d leaves were electroporated in a suspension buffer containing 1 mM $CaCl_2$ or 1 mM EGTA by square-wave pulse for 2 ms at 100, 75, or 50 V. After electroporation, survival was measured with fluorescein diacetate staining. Survival of untreated protoplasts at 0°C was taken as 100%. The values of survival are means ± SE (n = 3).

(B) Dehydration- and rehydration-induced stresses that are imposed during a freeze/thaw cycle were simulated by changes in osmotic concentration in the suspending medium. Protoplasts isolated from AC7d leaves were dehydrated by moving them from an isotonic solution (0.6 M sorbitol) to a hypertonic solution (2.15 M sorbitol) at 0°C in the presence of 1 mM $CaCl_2$ or 1 mM EGTA (left side). They were then rehydrated by returning them to the isotonic solution at 0°C (right side). Survival of untreated protoplasts at 0°C was taken as 100%. Data are means ± SE (n = 8). Asterisks indicate a statistically significant difference between calcium and EGTA treatments based on a Student's t test (*, $P < 0.05$; **, $P < 0.01$).

sections were frozen in the presence of a fluorescent probe, 2',7-biscarboxyethyl-5(6)-carboxyfluorescein (BCECF), in a solution containing 1 mM calcium. Because the fluorescent probes were found only in unfrozen water sites but not in ice crystals, ice crystals can be negatively observed under a fluorescence microscope (Neils and Diller, 2004). In addition, BCECF cannot pass through the plasma membrane. Before the solution in the absence of sorbitol was frozen, the fluorescence of BCECF, which is pseudocolored blue, was observed outside the tissue and in the intercellular space inside the tissue, but not in living cells of the leaf sections (yellow asterisks in Figure 6A show representative unfrozen sites). Once the solution was frozen, the fluorescence was rapidly excluded from the intercellular space (see Supplemental Figure 1 online). At −3°C, BCECF was concentrated in small spaces at the periphery of the section and some cells, or outside the tissue, but was not observed in large areas inside the tissue (Figure 6B). These results clearly indicate that ice crystals spread into the intercellular space inside the tissue (red asterisks in Figure 6B show representative frozen sites).

With a 0.6 M sorbitol solution, fluorescence distribution in tissues before freezing was the same as that in the absence of sorbitol (Figure 6D versus 6A). However, after the solution around the tissue was frozen, the fluorescence was observed not only outside, but also in the intercellular space inside the tissue (Figure 6C). In the tissue, cells and the intercellular space were distinguishable

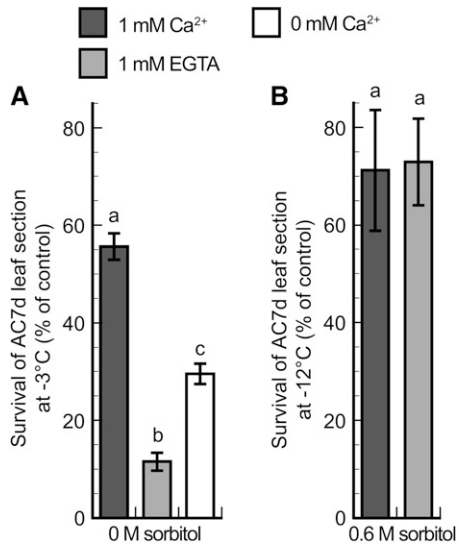

Figure 5. Extracellular Calcium-Dependent Freezing Tolerance of Leaf Sections.

Freezing tolerance was determined in leaf sections prepared from AC7d leaves. With a suspension buffer lacking sorbitol, freezing tolerance was measured after freezing to –3°C in the presence of 0 mM $CaCl_2$, 1 mM $CaCl_2$, or 1 mM EGTA **(A)**. With a suspension buffer containing 0.6 M sorbitol, freezing tolerance was measured after freezing to –12°C in the presence of 1 mM $CaCl_2$ or 1 mM EGTA **(B)**. Survival of unfrozen leaf sections at 0°C was taken as 100%. Data are means ± SE (n = 7 to 25). Different letters indicate statistically significant differences between treatments by one-way ANOVA with Tukey-Kramer multiple comparison test ($P < 0.05$).

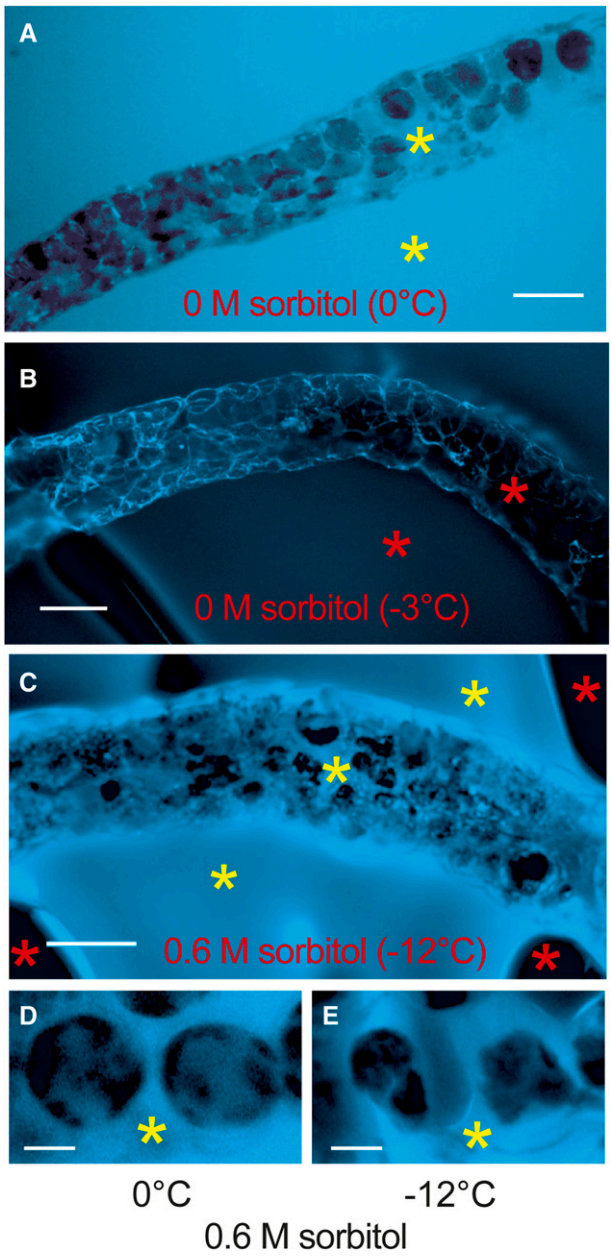

Figure 6. Ice Distribution Patterns in Leaf Sections.

Fluorescence microscopy images of the BCECF-stained sections before (**[A]** and **[D]**) and after freezing (**[B]**, **[C]**, and **[E]**) in a calcium-containing solution in the absence (**[A]** and **[B]**) or presence (**[C]** to **[E]**) of 0.6 M sorbitol were compared. Photos were taken before freezing in the absence of sorbitol **(A)**, after freezing at –3°C in the absence of sorbitol **(B)**, after freezing at –12°C in the presence of 0.6 M sorbitol **(C)**, before freezing in the presence of 0.6 M sorbitol **(D)**, and after freezing at –12°C in the presence of 0.6 M sorbitol **(E)**. Because the fluorescent probes are excluded from ice crystals, ice crystals appear as dark areas (Neils and Diller, 2004). In addition, because BCECF cannot pass through the plasma membrane, living cells also appear dark. The fluorescence of BCECF is pseudocolored blue. Yellow asterisks show representative sites of the unfrozen solution, and red asterisks show representative sites of the frozen solution. Bars = 100 μm in **(A)** to **(C)** and 20 μm in **(D)** and **(E)**.

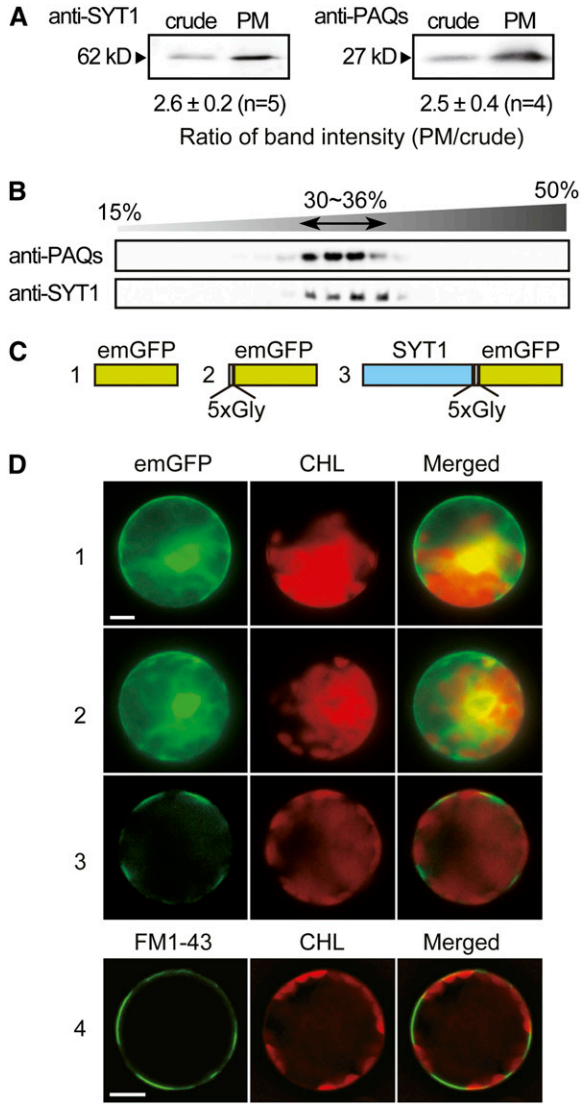

Figure 7. Subcellular Localization of SYT1.

(A) Purification of the plasma membrane with two-phase separation. The crude membrane fraction (4 μg) and the plasma membrane fraction (4 μg) were analyzed by immunoblotting with anti-SYT1 and anti-PAQs (plasma membrane maker). The protein amount in the plasma membrane fraction per the protein amount in the crude membrane fraction (i.e., purification rates after two phase separation) is shown at the bottom of each panel.

(B) Separation of crude membrane mixtures using linear sucrose density gradient centrifugation (15 to 50% [w/w]). Aliquots of each fraction were subjected to SDS-PAGE and analyzed by immunoblotting with anti-SYT1 and anti-PAQs.

(C) Diagram of GFP fusion proteins. (1) Control with GFP (green) only; (2) control with GFP with a flexible linker of penta-glycine (black) in the N terminus; (3) SYT1 (blue) conjugated to the GFP via the linker.

(D) Transient emGFP fusion protein expression assay. Plasmid DNA constructs containing emGFP (row #1), 5xGly-emGFP (row #2), or SYT1-5xGly-emGFP (row #3) under the control of the cauliflower mosaic virus 35S promoter were transfected into *Arabidopsis* mesophyll protoplasts isolated from nonacclimated leaves using polyethylene glycol, and then the emGFP signal and autofluorescence of chloroplasts were captured. The plasma membrane of protoplasts isolated from nonacclimated leaves was stained using 16 μM FM1-43 (row 4). Columns show the fluorescence from emGFP or FM1-43 (left), chlorophyll autofluorescence (CHL, middle), and the superimposed images (Merged, right). All photos are shown at the same scale; bar = 10 μm.

after freezing: cells were dark and the intercellular space was fluorescently bright, both of which remained unfrozen. Furthermore, cells in the tissue were apparently plasmolyzed (cf. Figures 6D with 6E), showing that the sorbitol solution is concentrated in the tissue. Under these conditions, the insides of all tissues observed in several experiments were not frozen during freezing. This means that freezing of a sorbitol solution results in an increase in the concentration of sorbitol in the unfrozen solution inside the tissues at subzero temperatures.

SYT1 Is Localized in the Plasma Membrane

Synaptotagmin VII has been reported to be involved in membrane resealing in animal cells (Reddy et al., 2001; Chakrabarti et al., 2003; Shen et al., 2005). Plant genomes contain synaptotagmin-like genes, and we identified a synaptotagmin-like protein (SYT1, previously referred to as AtSytA; 61.7 kD) as a cold-responsive plasma membrane protein in *Arabidopsis* (Kawamura and Uemura, 2003). The antibody against SYT1 was prepared using a peptide containing 16 amino acid residues of the C_2A domain of SYT1 (see Methods), and this antibody cross-reacted with a single band of 62 kD in plasma membrane and crude membrane fractions (Figure 7A). In addition, because no cross-reacting band was observed in the crude membrane fractions isolated from T-DNA mutants (see Supplemental Figure 2 online), we determined this anti-C_2A antibody to be specific for the C_2A domain of SYT1.

To determine whether SYT1 was localized mainly in the plasma membrane, the protein amount in the plasma membrane fraction per that in the crude membrane fraction (i.e., purification rates after two phase separation) were compared between SYT1 and plasma membrane aquaporins (PAQs) with immunoblot analysis. An antibody against PAQs that was raised against a common peptide sequence among six radish aquaporins (Ohshima et al., 2001) was used. This result showed that the purification rate of SYT1 was almost similar to that of PAQs (SYT1, 2.6; PAQs, 2.5) (Figure 7A). Next, crude membranes were separated using sucrose density gradient centrifugation. PAQs were detected in fractions containing 30 to 36% (w/w) sucrose (top panel in Figure 7B). The fractions in which SYT1 was detected were identical to those in which PAQs were detected (bottom panel in Figure 7B). Thus, both results show that two physical features (that is, surface charge and density) of the membrane to which SYT1 belongs are almost similar to those of the membrane to which PAQs belong.

Second, the in vivo localization of SYT1 was confirmed by transient expression of the *SYT1* gene conjugated to synthetic green fluorescent protein (emGFP) via penta-glycine as a flexible linker in protoplasts isolated from nonacclimated *Arabidopsis* leaves (Figure 7B). When emGFP or emGFP with penta-glycine at

the N terminus was expressed in protoplasts as a control, emGFP fluorescence was detected both in the cytosol and nucleus (rows 1 and 2 in Figure 7C). On the other hand, fluorescence of SYT1-emGFP fusion proteins was detected only at the peripheral region of protoplasts (row 3 in Figure 7C). In addition, the fluorescence image of SYT1-emGFP fusion proteins was similar to that of the plasma membrane that was stained by 16 μM FM1-43 (cf. rows 3 and 4 in Figure 7C) (Yamazaki et al., 2008). Collectively, the results of Figure 7 show that SYT1 is localized mainly in the plasma membrane in *Arabidopsis* mature leaves.

Anti-SYT1 Antibody Inhibits Calcium-Dependent Freezing Tolerance

We studied the effect of anti-SYT1 antibody on calcium-dependent freezing tolerance using leaf sections prepared from AC7d leaves (Figure 8A). The addition of anti-SYT1 antibody (final concentration of 0.13 μM) resulted in mitigation of calcium-dependent freezing tolerance and a decrease in survival to 34% (lane 1 in Figure 8A), which was similar to the freezing tolerance in the absence of calcium (26%) (lane 2 in Figure 8A). On the other hand, when a mixture of antibody and antigen peptide (final concentration of 0.13 and 1 μM, respectively) was added into the sample solution, survival (53%) was similar to that in the presence of calcium alone (61%) (lanes 3 and 4 in Figure 8A) and much greater than that either in the absence of calcium or in the presence of calcium and anti-SYT1 antibody. Because immunoblot analysis of the plasma membrane fraction with a mixture of the antibody and antigen showed no proteins that cross-reacted with the mixture (Figure 8B), calcium-dependent freezing tolerance is likely related to the function of the C_2A domain of SYT1.

Because the C_2A domain of animal synaptotagmin exists in the cytoplasmic region (for review, see Bai and Chapman, 2004), the results of Figure 8A suggest that SYT1 functions after the plasma membrane is punctured. Thus, we determined the topology of the C_2A domain of SYT1 using freshly prepared plasma membrane fractions from nonacclimated *Arabidopsis* leaves, which mainly contained sealed right-side-out vesicles (Palmgren et al., 1990). The plasma membrane fractions were treated by thermolysin with or without 1% (w/v) Triton X-100 for 1 h at 4°C and then analyzed by immunoblot analysis with anti-SYT1 antibody. Without Triton X-100, there was no effect of thermolysin treatment on the detected band (top panel in Figure 8C). With Triton X-100, however, the detected band gradually disappeared as the concentration of thermolysin increased (bottom panel in Figure 8C). Thus, these results show that the C_2A domain in SYT1 is exposed on the cytosolic side of the plasma membrane.

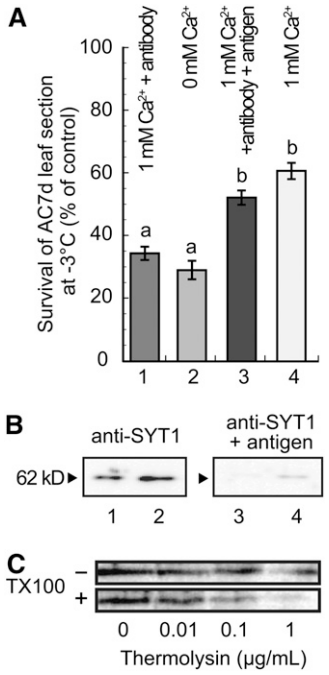

Figure 8. Synaptotagmin-Associated Membrane Resealing.

(A) In a suspension buffer without sorbitol, freezing tolerance of leaf sections isolated from AC7d plants was measured after freezing to –3°C in the presence of 1 mM $CaCl_2$ and 0.13 μM anti-SYT1 antibody (lane 1), 0 mM $CaCl_2$ (lane 2), 1 mM $CaCl_2$, 0.13 μM anti-SYT1 antibody, and 1 μM antigen peptide (lane 3), or 1 mM $CaCl_2$ (lane 4). Data are means ± SE (n = 20 to 40). Different letters indicate statistically significant differences between treatments by one-way ANOVA with Tukey-Kramer multiple comparison test ($P < 0.05$).

(B) Immunoblot analysis was performed with 1 μg (lanes 1 and 3) or 2 μg (lanes 2 and 4) proteins of plasma membrane fraction prepared from AC7d leaves using the anti-SYT1 antibody (lanes 1 and 2) or a mixture of the antibody and the antigen (lanes 3 and 4).

(C) Fresh plasma membrane fractions containing 2 μg of proteins in 100 μL were treated by thermolysin (final concentrations of thermolysin were 0, 0.01, 0.1, and 1 μg mL^{-1}) with or without 1% (w/v) Triton X-100 for 1 h at 4°C. After the reactions were stopped by adding 1 μL of 0.5 M EGTA, samples were analyzed by immunoblot using antibodies against the C_2A domain of SYT1. We performed this experiment twice, and we got similar results in both.

Disappearance of Calcium-Dependent Freezing Tolerance in *SYT1*-RNAi Mutants

The expression of the *SYT1* gene during cold acclimation was analyzed by real-time RT-PCR analysis. The expression level of *SYT1* in leaves rapidly increased (1.8-fold) after 1 d of cold acclimation, reached the maximal level (2.1-fold) after 3 d of cold acclimation, and then slightly decreased after 7 d of cold acclimation (Figure 9A). Thus, *SYT1* is a cold-inducible gene, while the expression pattern of *SYT1* was different from that of *RD29A* (Figure 9B), which contains a C repeat/dehydration-responsive element (Yamaguchi-Shinozaki and Shinozaki, 1994). In fact, the PLACE program (http://www.dna.affrc.go.jp/PLACE/) showed that the nucleotide sequences of the upstream from the start codon of *SYT1* gene to the next gene upstream (At2g20980) had no C repeat/dehydration-responsive element.

We next constructed *Arabidopsis* RNAi mutants to study the relationship between SYT1 and freezing tolerance. RNAi constructs, in which the antisense and sense DNA fragment containing the 3′ untranslated region (UTR) of *SYT1* or full-length *GFP* (for control) were linked with a β-glucuronidase (GUS) fragment downstream of the *RD29A* promoter, were introduced into *Arabidopsis* (Figure 10A). Two *SYT1*-RNAi lines with reduced

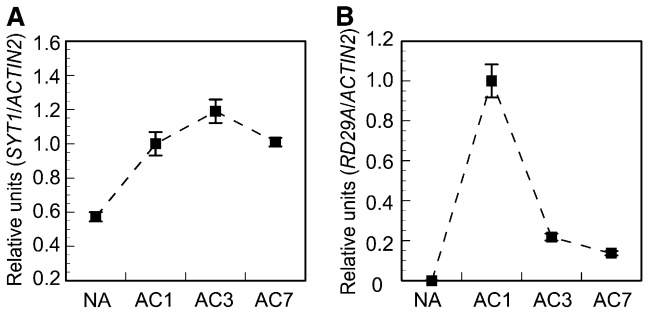

Figure 9. Real-Time PCR Analysis of *SYT1* Expression.

Total RNA was isolated from nonacclimated (NA), or 1-d (AC1d), 3-d (AC3d), or 7-d (AC7d) cold-acclimated leaves. The expression of *SYT1* **(A)** and *RD29A* **(B)** was detected by real-time RT-PCR. Expression level of *ACTIN2* gene was used as an internal control. Expression levels were normalized to that in the AC1d sample, and the data are expressed as relative values. Data are means ± SD (n = 3).

expression of *SYT1* (#13 and #47) and two control *GFP*-RNAi lines (#6 and #7) were identified by RT-PCR. With both nonacclimated and AC3d seedlings, real-time PCR experiments showed that the expression levels of *SYT1* in the two *SYT1*-RNAi lines were much lower than those in the two control lines, which were almost the same level as that observed in wild-type plants (Figure 10B). Immunoblot analysis revealed that SYT1 signals in the plasma membranes of *SYT1*-RNAi lines #13 and #47 before cold acclimation were ~40 and 80% lower, respectively, than those in the two control lines (Figure 10C). After 7 d of cold acclimation, the signals increased in all samples, but were still less in RNAi mutants than wild-type plants.

Survival of protoplasts prepared from control and *SYT1*-RNAi lines after 7 d of cold acclimation was then measured after freezing to –8°C in the presence of calcium or EGTA. In the presence of 1 mM calcium, the survivals of control lines (#6, 72%; #7, 66%) were significantly higher than those of *SYT1*-RNAi lines (#13, 49%; #47, 46%) (Figure 11A). On the other hand, in the presence of 1 mM EGTA, the survivals of control lines (#6, 43%; #7, 36%) were almost similar to those of *SYT1*-RNAi lines (#13, 41%; #47, 36%) (Figure 11B). Furthermore, calcium-dependent enhancement of protoplast survival also disappeared in *SYT1*-RNAi mutants subjected to electroporation (see Supplemental Figure 3 online). Thus, these results indicate that the calcium-dependent enhancement of the freezing tolerance of protoplasts is due to SYT1-dependent plasma membrane resealing of damage caused by mechanical stress.

The involvement of SYT1 in the calcium-dependent freezing tolerance of walled cells was evaluated by determination of the freezing tolerance of leaf sections prepared from the control and *SYT1*-RNAi lines in a solution without sorbitol. In the presence of 1 mM calcium, the survivals of control lines (#6, 55%; #7, 54%) were significantly higher than those of *SYT1*-RNAi lines (#13, 35%; #47, 39%) (Figure 12A). On the other hand, in the absence of calcium, the survivals of control lines (#6, 25%; #7, 30%) were almost similar to those of *SYT1*-RNAi lines (#13, 28%; #47, 24%) (Figure 12B). Thus, the calcium-dependent freezing tolerance of intact leaf sections (that is, cells with cell walls) was apparently lost in *SYT1*-RNAi lines.

Freezing Tolerance of *SYT1*-RNAi and T-DNA Insertion Mutants in Whole Plants or Whole Leaves

Finally, we checked the effect of *SYT1* reduction on freezing tolerance using whole plants or whole leaves. When whole plants of RNAi lines grown on agar plates were frozen at −10°C for 12 h, survival was determined by measuring regrowth ability at 10 d after freezing. The number of surviving plants of *SYT1*-RNAi line #47 was lower than that of control lines #6 and #7 (Figure 13A, Table 1). On the other hand, *SYT1*-RNAi line #13 was as freezing tolerant as control lines (Table 1), perhaps because the suppression of *SYT1* was weaker in line #13 than in line #47 (Figure 13B, Table 1). Next, a T-DNA insertion line for *SYT1* was used (see mutant information in Supplemental Figure 2 online). The number of surviving plants of T-DNA mutants was apparently lower than the number of wild-type plants (Figure 13B, Table 1). In addition, when electrolyte leakage (EL), as an index of plasma membrane injury (Levitt, 1980), was measured in leaves from the RNAi lines, T-DNA mutants, and wild-type plants, EL values increased linearly from −8 to −14°C, with maximum values observed at −14°C. However, the EL values of *SYT1*-RNAi line #47 or T-DNA mutants were statistically higher than those of control line #7 or

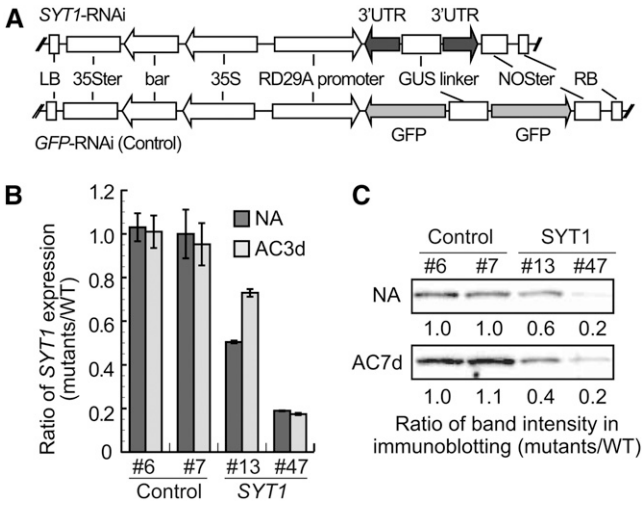

Figure 10. *Arabidopsis* Mutants in Which the Expression Level of *SYT1* Is Decreased by the Expression of RNAi.

(A) In RNAi constructs, the antisense and sense DNA fragments containing the 3′ UTR of *SYT1* (top) or full-length *GFP* (bottom) were linked with a GUS fragment downstream of the *RD29A* promoter (see Methods).

(B) The expression levels of *SYT1* in the two *SYT1*-RNAi lines, nonacclimated (NA) or cold-acclimated for 3 d (AC3d), were determined by real-time PCR. Data are means ± SD (n = 3).

(C) Immunoblot analyses using anti-SYT1 antibody were performed with 1 μg of protein from plasma membrane fractions prepared from leaves of RNAi lines that were nonacclimated (NA) or cold-acclimated for 7 d (AC7d). The band intensity of control line #6 was taken as 1.0 and is shown at the bottom of each determination.

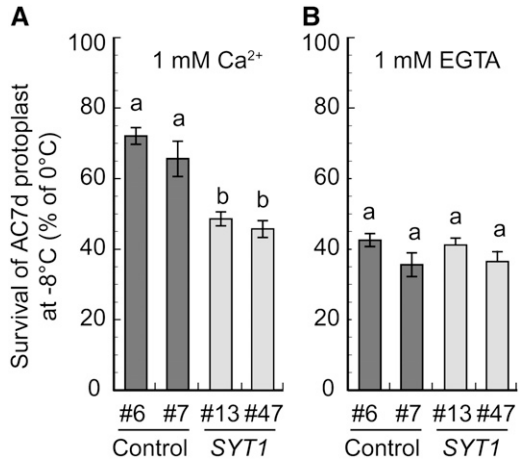

Figure 11. Extracellular Calcium-Dependent Freezing Tolerance of Protoplasts Isolated from RNAi Lines.

Freezing tolerance of protoplasts isolated from AC7d control plants (black bars; #6 and #7) and *SYT1*-RNAi lines (white bars; #13 and #47) was determined in the presence of 1 mM $CaCl_2$ **(A)** or 1 mM EGTA **(B)**. Survival was measured after freezing to –8°C. Survival of unfrozen protoplasts that were kept at 0°C was taken as 100%. Data are means ± SE (n = 10). Different letters indicate statistically significant differences between treatments by one-way ANOVA with Tukey-Kramer multiple comparison test ($P < 0.05$).

wild-type plants at −10 and −12°C (Figure 13C). Thus, SYT1 reduction induced a decrease in freezing tolerance in *Arabidopsis* at the whole plant level.

DISCUSSION

Freezing Tolerance Is Enhanced by Membrane Resealing

This study was planned to test the hypothesis that freezing tolerance involves calcium-dependent membrane resealing when the plasma membrane is punctured by freeze-induced mechanical stress. A membrane resealing process that depends on the influx of extracellular calcium into the cytoplasm at the damaged plasma membrane site has been shown in animal cells. Thus, if plant cells possess a membrane resealing system like that of animal cells, the survival of cells that have suffered mechanical damage to the plasma membrane must be affected by extracellular calcium. In this study, we demonstrated that, at both the cell and tissue levels, calcium-dependent freezing tolerance accounts for ~40 to 60% of the enhanced freezing tolerance after cold acclimation (Figures 1 and 5A). Because survival gradually increased at 0.25 mM $CaCl_2$ or higher, and reached a maximum at 1 mM (Figure 2A), the enhancement of freezing tolerance could be calcium dependent under physiological calcium concentrations in apoplasts, believed to be millimolar levels (Hepler and Wayne, 1985). Calcium enhanced the tolerance to electroporation in protoplasts (Figure 4A).

This is of interest because, in mammalian cells, the tolerance to electroporation-induced mechanical stress is associated with membrane resealing (Huynh et al., 2004). In theory, electroporation induces the formation of pores in the plasma membrane (Freeman et al., 1994); indeed, electroporation-induced pores have been observed by electron microscopy after electroporation (Chang and Reese, 1990). On the other hand, the tolerance of protoplasts to dehydration and rehydration is not dependent on extracellular calcium (Figure 4B). These results collectively indicate that extracellular calcium is needed for plant cells to enhance their tolerance to freeze-induced mechanical stress, but not for tolerance to dehydration- and rehydration-induced mechanical stresses occurring during the freeze/thaw process.

In mammalian cells, after the plasma membrane is damaged, synaptotagmin VII is thought to recognize the calcium influx from the extracellular space and commence the membrane resealing event (Reddy et al., 2001; Chakrabarti et al., 2003; Shen et al., 2005). In addition, the synaptotagmin-like protein SYT1 is a cold-responsive plasma membrane protein in *Arabidopsis* (Kawamura and Uemura, 2003). Thus, SYT1 is a key protein to understand the role of membrane resealing in freezing tolerance. Calcium-dependent freezing tolerance was significantly decreased in the presence of the antibody against C_2A domain of SYT1 (lane 1 in Figure 8A). Considering that the C_2A domain exists in the cytoplasmic region (Figure 8C), the plasma membrane must be punctured during freeze/thawing process to allow the antibody to flow from the extracellular space to the cytoplasm at the damaged sites on the plasma membrane and bind to the C_2A domain of SYT1 in the cell, resulting in dysfunction of SYT1 in calcium-dependent membrane resealing. Conversely, when calcium-dependent freezing tolerance is observed, the punctured

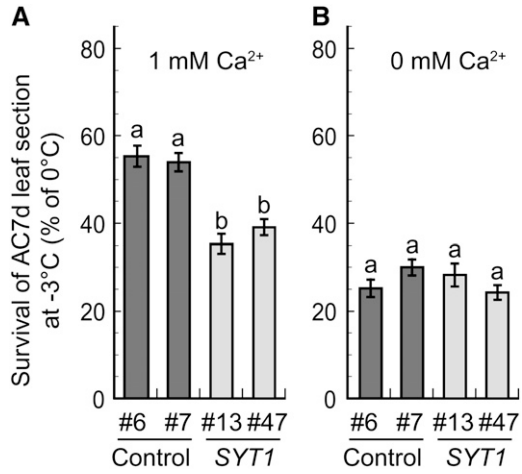

Figure 12. Extracellular Calcium-Dependent Freezing Tolerance of Leaf Sections Isolated from RNAi Lines.

Freezing tolerance of leaf sections prepared from AC7d control plants (black bars; #6 and #7) and *SYT1*-RNAi lines (white bars; #13 and #47) was determined in the presence of 1 mM $CaCl_2$ **(A)** or 1 mM EGTA **(B)**. In a solution without sorbitol, survival was measured after freezing to –3°C. Survival of unfrozen leaf sections at 0°C was taken as 100%. Data are means ± SE (n = 30 to 60). Different letters indicate statistically significant differences between treatments by one-way ANOVA with Tukey-Kramer multiple comparison test ($P < 0.05$).

Table 1. Freezing Test at the Whole-Plant Level

	Control		*SYT1*-RNAi	
	#6	#7	#13	#47
Survival (%)	73 ± 8^{ab}	78 ± 8^{a}	80 ± 7^{a}	40 ± 11^{b}
	Wild type		T-DNA	
Survival (%)	73 ± 8^{a}		38 ± 11^{b}	

Regrowth assay was performed as shown in Figures 13A and 13B. Plants were grown on Murashige and Skoog medium containing 0.8% agar in a square dish. Ten-day-old plants of RNAi-expressing lines, wild-type plants, and T-DNA mutants were cold-acclimated for 7 d. The plates were exposed to –10°C in a programmable freezer for 12 h and thawed at 2°C. Pictures were taken after 10 d, and then living plants were counted. Data are means ± SE (n = 5). Different letters indicate statistically significant differences between treatments by one-way ANOVA with Tukey-Kramer multiple comparison test ($P < 0.05$).

site must be resealed. Thus, the fact that calcium-dependent freezing tolerance is observed again when the activity of the anti-SYT1 antibody is inhibited by preincubation with its antigen (lane 3 in Figure 8A) cannot be explained by hypotheses other than membrane resealing.

Second, genetic studies revealed that the effect of calcium on tolerance to freezing or electroporation disappeared in protoplasts and leaf sections prepared from *SYT1*-RNAi lines (Figures 11 and 12; see Supplemental Figure 3 online), providing strong evidence that SYT1 is involved in the calcium-dependent tolerance to mechanical stresses. Interestingly, it has been reported that the *syt1* mutant of *Arabidopsis* decreases the integrity of the plasma membrane (Schapire et al., 2008). Thus, we conclude that calcium-dependent freezing tolerance results from the membrane resealing of plasma membrane damage occurring during freeze/thawing and that the mechanism involves SYT1 function.

Predicted Function of SYT1

Synaptotagmins interact with membranes composed of negatively charged phospholipids at C_2A and C_2B domains, and this interaction is mediated by calcium (Bai and Chapman, 2004; Stein et al., 2007), which triggers calcium-dependent exocytosis (Schonn et al., 2008). The structural features of mammalian synaptotagmins include a transmembrane domain at the N terminus and two tandem calcium binding C_2A and C_2B domains at the C terminus, both of which are conserved in SYT1 (Kawamura and Uemura, 2003). Because of these structural similarities, it is expected that SYT1 may function as a calcium sensor in exocytosis. In fact, it has been confirmed that phospholipid binding activities of two C2 domains in *Arabidopsis* SYT1 are regulated by calcium concentration (Schapire et al., 2008). It seems that the subcellular localization of synaptotagmins is not the same in living organisms. Synaptotagmin VII, which is the most homologous to SYT1 among mammalian synaptotagmins, is primarily localized in endomembranes, but not in the plasma membrane (Fukuda et al., 2004). On the other hand, the yeast synaptotagmin homolog Tcb3 is localized in the plasma membrane as is SYT1, and genetic evidence indicates that Tcb3 may be involved in membrane resealing during mating (Aguilar et al., 2007). The biochemical and genetic analyses in this study revealed that SYT1 is in fact localized predominantly in the plasma membrane in leaves (Figure 7). This result is consistent with those in our previous study in which SYT1 was identified

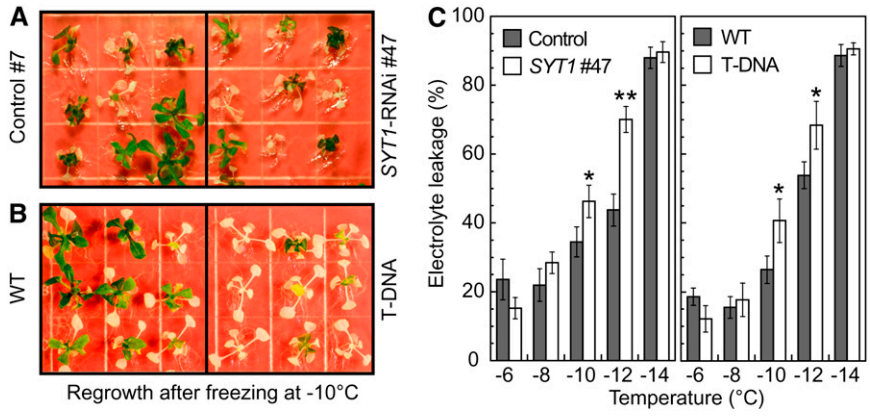

Figure 13. Involvement of Synaptotagmin in Plant Freezing Tolerance.

(A) and **(B)** Regrowth assay after freeze/thawing. Plants were grown on Murashige and Skoog medium containing 0.8% agar in a square dish. Ten-day-old plants of RNAi lines **(A)** or wild-type plants and T-DNA mutants **(B)** were cold-acclimated for 7 d and then exposed to –10°C in a programmable freezer for 12 h. After plants were thawed at 2°C and then kept at 23°C for 10 d, pictures were taken.

(C) Electrolyte leakage analysis. RNAi lines, wild-type plants, and T-DNA mutants were grown on soil for 4 weeks and then cold-acclimated for 7 d. Electrolyte leakage from the leaves of each plant was measured after freeze/thawing of samples. Control line #7 (black bars) and *SYT1*-RNAi line #47 (white bars) are shown in the left panel, while a wild-type plant (black bars) and T-DNA mutant (white bars) are shown in the right panel. Data are means ± SE (n = 7 to 10). Asterisks indicate a significant difference from the values of the control line or wild-type plant based on a Student's t test (*, $P < 0.05$; **, $P < 0.01$).

in the highly purified plasma membrane fraction in *Arabidopsis* (Kawamura and Uemura, 2003). While the subcellular localization of synaptotagmin may change during divergence of eukaryotes, it is possible that synaptotagmin function in calcium sensing and calcium-dependent membrane resealing is conserved in eukaryotes.

SYT1 belongs to a small gene family, and the *Arabidopsis* genome contains five genes encoding synaptotagmin-like proteins (*SYT1*, At2g20990; *SYT2*, At1g20080; *SYT3*, At5g04220; *SYT4*, At5g11100; *SYT5*, At1g05500; previously named *AtSytA-E*, respectively, by Craxton, 2004). Our sequence data analysis of these genes collected from The Arabidopsis Information Resource database (http://www.Arabidopsis.org/) revealed that the full-length cDNA encoding *SYT3* (accession number AY059741; BX830716) has a stop codon in the coding sequence, indicating that *SYT3* is actually a pseudogene. The deduced amino acid sequence of SYT1 shares 66% identical amino acid residues with SYT2 but only 30% with SYT4 and SYT5. RT-PCR did not detect expression of *SYT2* or *SYT4* in either nonacclimated or cold-acclimated seedlings (see Supplemental Figure 4A online), which agrees with the microarray database (http://bbc.botany.utoronto.ca/efp/cgi-bin/efpWeb.cgi) that high expression of *SYT2* or *SYT4* is detected especially in pollen or dry seeds. The *SYT5* expression level increased after 1 d of cold acclimation, but the expression level was not maintained during cold acclimation (see Supplemental Figure 4B online). Thus, the expression pattern and amino acid sequence of *SYT5* was different from those of *SYT1*, implying their functional differentiation in cold acclimation or freezing tolerance in leaves.

Membrane Resealing May Work against the Mechanical Stress Associated with Ice Crystal Growth

Mechanical stress during a freeze/thaw cycle is induced by freeze-induced dehydration, thaw-induced rehydration, and ice crystal growth (Levitt, 1980). Which of these conditions triggers calcium-dependent membrane resealing is unclear. Calcium-dependent tolerance apparently occurred in protoplasts subjected to mechanical stress by electroporation (Figure 4A) but was scarcely observed when protoplasts were subjected to only osmotic stress (Figure 4B). This is consistent with the results obtained with leaf sections: as shown in Figure 5B, calcium-dependent freezing tolerance did not occur when leaf sections were immersed in a sorbitol solution. In this case, plant cells in leaf sections may suffer only dehydration-induced osmotic stress but not mechanical stress during freeze-induced ice crystal growth (Figures 6C and 6E). On the other hand, if cells in leaf sections that were immersed in a solution without sorbitol directly suffered from mechanical stress associated with ice crystal growth during freezing (Figure 6B; see Supplemental Figure 1 online), calcium-dependent freezing tolerance became evident (Figure 5A). These results collectively suggest that membrane resealing during freeze/thawing may counteract the mechanical damage to the plasma membrane associated with ice crystal growth.

How does ice crystal growth damage the plasma membrane? One possibility is the pressure against the cell caused by ice crystal growth. For example, the plasma membranes of plant cells sandwiched between ice crystals may be mechanically pressed when each ice crystal grows. In electron microscopy studies, plant cells in tissue have been observed to be mechanically deformed by the extracellular ice crystals (Pearce, 1988; Pearce and Ashworth, 1992; Fujikawa et al., 1999). Another possibility is that the damage is due to excess adhesion between ice and the plasma membrane during a freeze/thaw cycle. It has been hypothesized that adhesion energy develops between ice and hydrophilic polymers during freezing as they compete for liquid water and that the ice adhesion eventually results in damage to the plasma membrane (Olien, 1974; Olien and Smith, 1977).

Endomembranes are necessary for the membrane resealing system that is used to withstand mechanical stresses (Bi et al., 1995). In fact, it has been reported that the number of microvesicles that are formed from fragmentation of the endoplasmic reticulum increases in the vicinity of the plasma membrane during cold acclimation in plants, including *Arabidopsis* (Ristic and Ashworth, 1993). While the role of these microvesicles is not yet determined, it is possible that microvesicles function in a membrane resealing system together with SYT1, which exists in the plasma membrane. Recently, we found that many

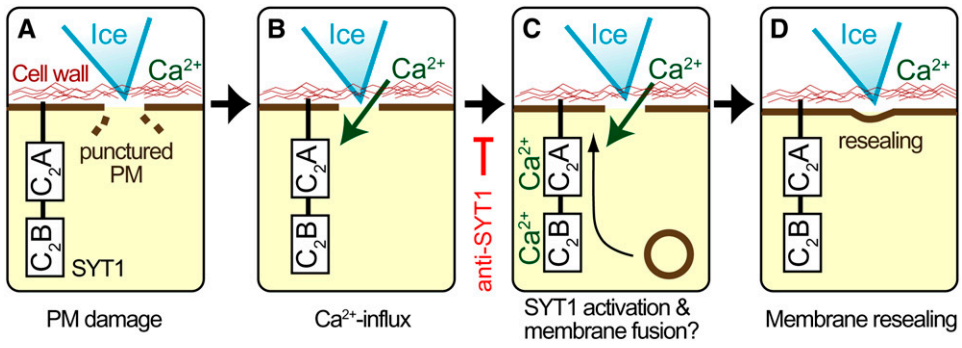

Figure 14. A Proposed Model for Calcium- and SYT1-Induced Membrane Resealing Occurring during Freeze/Thawing.

The plasma membrane is mechanically punctured by ice crystals **(A)**. Subsequently, calcium influx occurs from the extracellular space into the cytoplasm through the damaged sites **(B)**; endomembranes may then fuse at the site of the damaged plasma membrane via calcium binding SYT1 **(C)**, and, consequently, the damaged site is resealed **(D)**.

freeze-induced vesicular structures (FIVs) appeared in the cytoplasmic region near the plasma membrane just after extracellular freezing occurred in *Arabidopsis* protoplasts isolated from cold-acclimated leaves (Yamazaki et al., 2008). We concluded that FIV formation is associated with surface area regulation (SAR), by which plant cells loosen the mechanically stressful deformation of the plasma membrane induced by ice crystal growth during freezing (Yamazaki et al., 2008). Although the molecular mechanism underlying SAR is still unknown, SAR is simply stated as follows: surface area is added locally from endomembranes when the tension of the membrane increases locally, and, vice versa, a local decrease in plasma membrane tension leads to the localized retrieval of excess surface area (Mills and Morris, 1998; Raucher and Sheetz, 1999; Morris and Homann, 2001). Thus, SAR is an event that circumvents plasma membrane damage, while membrane resealing is an event that occurs after membrane damage. Interestingly, we also observed that FIVs occasionally fused with the plasma membrane (Yamazaki et al., 2008). While it is possible that this fusion results from SAR to relax the stress upon the plasma membrane during freezing, it is also possible that FIVs may be used for membrane resealing.

The Role of Membrane Resealing in the Freezing Tolerance of Intact Tissue

While the calcium-dependent freezing tolerance of protoplasts was observed throughout the temperature range tested in this study (Figure 1), the decrease in freezing tolerance of whole leaves isolated from SYT1-defective mutants was observed only at −10 and −12°C (Figure 13C). Because membrane resealing may work when plant cells directly suffer from mechanical stress associated with ice crystal growth, as described above, it is possible that the ice nucleation and ice distribution in apoplasts are managed in plants to avoid the close proximity of ice to cells, and, consequently, membrane resealing does not function in whole plants until the ice management system in apoplasts is broken. In fact, it is known that ice nucleation, ice distribution, and ice crystal growth are complexly managed in some organs (for example, leaves and flower buds) in plants, including *Arabidopsis* (Ishikawa et al., 1997; Ide et al., 1998; Griffith et al., 2005; Reyes-Diaz et al., 2006).

Interestingly, survival of leaf sections frozen in the presence of 0 mM calcium was somewhat higher than that in the presence of EGTA (Figure 5A), which is different from the results obtained with protoplasts (Figure 2A). This result leads us to the idea that cell walls may protect plant cells against mechanical stress induced by freezing. This is partly because the mechanical resistance of cell walls decreases following the addition of a calcium chelator, which removes pectin from cell walls (Ezaki et al., 2005). This idea is also indirectly supported by the fact that the quantitative and qualitative features of pectin change during cold acclimation (Solecka et al., 2008). Thus, to better understand the mechanism underlying freezing tolerance at the whole-plant level, it will be necessary to determine the relationships among ice management, cell wall properties, and membrane resealing.

Finally, our results collectively suggest that SYT1 is involved in the resealing of the plasma membrane damaged due to freeze-induced mechanical stress. In detail, after ice crystals spread in the extracellular space and press on cells, the plasma membrane is mechanically punctured (Figure 14A). Subsequently, calcium influx from the extracellular space into the cytoplasm through the damaged sites occurs (Figure 14B), and endomembranes may then be fused at the site of the damaged plasma membrane via calcium binding SYT1 (Figure 14C).These events eventually seal the damaged site (Figure 14D) and decrease the occurrence of freezing injury. Our results provide novel information on the effect of mechanical stress induced by ice crystal growth on plant cell survival during a freeze/thaw cycle.

METHODS

Plant Materials

Seeds of *Arabidopsis thaliana* (Columbia) were planted and grown as previously described (Uemura et al., 1995) with a slight modification of light conditions (16-h photoperiod at 125 μmol/m^2/s at soil level). Non-acclimated plants were kept in this environment for 24 d. Cold acclimation was achieved by subjecting 24-d-old plants to a temperature of 2°C (12-h photoperiod at 125 μmol/m^2/s at soil level) for 1 to 7 d. A plasmid clone of the full-length cDNA of *SYT1* (MIPS code At2g20990, cDNA clone name RAFL05-21-F01) was obtained from the RIKEN BioResource Center (Seki et al., 1998, 2002b).

RNA Expression Analysis

Total RNA was extracted from 4-week-old plants using the NucleoSpin RNA II RNA isolation kit (MACHEREY-NAGEL). For RT-PCR analysis, reverse transcription was performed using the RevatraAce kit (TOYOBO) according to the product manual. PCR was performed using ExTaq (TaKaRa Bio) with the following conditions: denaturing template DNA, 94°C, 15 s; annealing primer, 55°C, 30 s; and extension reaction, 72°C, 30 s; 30 cycles. PCR products were fractionated by agarose electrophoresis and detected by ethidium bromide staining. The following primer sets were used (and also for real-time PCR): *SYT1* (5′- AAATGGTGCCTGACGAACAT-3′ and 5′- CCTCCAGCTTCCCCCTATAC-3′ or 5′-CTGCACGTTGAAGTGCTGAG-3′ and 5′-CGATTTGGATCTTTCCGTTC-3′), *RD29A* (5′-CGGTGCAGAAGGAGCTTTAA-3′ and 5′- CTGGTATGGAGGAACTTCTTAATCC-3′), and *ACTIN2* (5′-CTAAGCTCTCAAGATCAAAGGCTTA-3′ and 5′-ACTAAAACGCAAAACGAAAGCGGTT-3′).

Real-time RT-PCR analysis was performed using a One-Step SYBR Prime Script RT-PCR kit (TaKaRa Bio) according to the product manual. Extracted total RNA was amplified using the Thermal Cycler Dice Real Time system (TaKaRa Bio). From the obtained data, a second derivative maximum was calculated, and the amount of template RNA was determined using a standard curve for each primer set. To compare the relative amounts of different samples, each value was normalized to the expression level of the *ACTIN2* gene as an internal control (Thorlby et al., 2004; Nicot et al., 2005). Gene-specific primer sets for each gene were designed using Primer3 online software (http://frodo.wi.mit.edu/). The specificities of these primer sets were checked by comparing their sequences with other homologous genes. This experiment was performed three times, and the mean values were calculated.

RNAi Mutants

The *RD29A* promoter region (Yamaguchi-Shinozaki and Shinozaki, 1994), the 3′ UTR of the *SYT1* gene, and the *GFP* gene were amplified by PCR using KOD plus (TOYOBO) according to the product manual using the

following primer sets: 3′ UTR of *SYT1*, 5′-TTTCTGAGTTGATTCGAG-3′ and 5′- GGCAAATCTGAATGTTGG-3′; *GFP*, 5′-ATGGTGAGCAAGGGC-GAG-3′ and 5′-ATGGACGAGCTGTACAAGGAAAACCTGTATTTT-CAGGGC-3′. The PCR products were subcloned, and their sequences were confirmed. The *RD29A* promoter region was ligated into the *Hin*dIII/*Eco*RI site in the multiple cloning site of a binary vector, pCAMBIA3300 (http://www.cambia.org), which contains a chemical herbicide BASTA-resistant gene (*bar*). Then, downstream of the *RD29A* promoter, the antisense and sense DNA fragments of *SYT1* 3′ UTR or full-length *GFP* were linked to a GUS fragment as a linker fragment (Figure 6A). The constructs were introduced into the *Arabidopsis* genome by *Agrobacterium tumefaciens*. Seeds of T1 plants were planted on soil and selected with 0.01% glufosinate ammonium (BASTA), and the transformed plants containing the constructs were checked by genomic PCR to amplify the *bar* fragment. In these transformed plants, the reduction of *SYT1* expression was checked first by RT-PCR and then confirmed by real-time RT-PCR using the primer set described above. Seeds of these RNAi lines (T3 plants) were planted on Murashige and Skoog medium with 0.8% agar, and plants were then transferred to soil after 10 d and grown for 4 weeks under the light conditions described above.

T-DNA Insertion Line

Seeds of plants with the T-DNA tag in the SYT1 locus (SAIL775A08) were obtained from the SAIL T-DNA collection. These plants were once backcrossed with wild-type plants, and heterozygous lines (B1 plants) were identified by genomic PCR using several sets of specific primers. The nucleotide sequences of the primers used are as follows: RP 5′-GCCTCCTGACAAGTATAGGGG-3′; LP, 5′-AGGTCTCGCGATTTAT-TAGGG-3′; RB, 5′-ATTAGGCACCCCAGGCTTTACACTTTATG-3′; barF, 5′-GCACCATCGTCAACCACTAC-3′; barR, 5′-GTACCGGCAGGCT-GAAGTC-3′; and 21000, 5′-AGGCGAGAACGTCAGCTTTA-3′. The amplified PCR products were sequenced. From B2 plants, homozygous lines were identified by genomic PCR. In addition, the expression of the *SYT1* gene and the accumulation of SYT1 in the crude membrane fraction of the homozygous line were checked by RT-PCR and immunoblot analysis, respectively.

Transient GFP Fusion Protein Expression Assay

The coding sequence of *SYT1* was amplified using KOD Plus (TOYOBO) with a primer set (5′-TACGCGTCGACATGGGCTTTTTCAGTACG-3′ and 5′-TACATGCCATGGCGCCGCCACCACCTCCGGCAGTTCGCCACTC-GAA-3′), inserted into a directional cloning vector, pENTR (Invitrogen), and then sequenced. To improve GFP fluorescence, the N terminus of emGFP (Invitrogen) was attached to the C terminus of SYT1 via the linker penta-glycine. The sGFP (S65T) gene in a conventional GFP expression vector (Niwa et al., 1999) was altered to the gene emGFP, with or without the penta-glycine in the N terminus, and then the DNA fragment coding *SYT1* was inserted into the *Sal*I/*Nco*I site of the vector. Using standard polyethylene glycol transfection methods, 10 μg of plasmid DNA of each construct was transfected into 2×10^4 protoplasts isolated from non-acclimated leaves in 100 μL of transfection buffer, and then GFP expression was observed after overnight incubation. For the observation of emGFP fluorescence and autofluorescence of chlorophylls in chloroplasts, filter sets of U-MNIBA2 and U-MWIG2 (Olympus) were used, respectively.

Visualization of the Plasma Membrane of Protoplasts

The plasma membrane of protoplasts isolated from nonacclimated leaves was stained using a lipophilic fluorescent dye of 16 μM FM1-43 (Molecular Probes) according to the method of Yamazaki et al. (2008). For the observation of FM1-43 fluorescence, a filter set of U-MNIBA2 (Olympus) was used.

Isolation of Protoplasts and Stress Tolerance Tests

Protoplasts were enzymatically isolated from either nonacclimated or cold-acclimated leaves according to the method previously described (Uemura et al., 1995). Isolated protoplasts were then suspended in a 0.4 M (nonacclimated), 0.5 M (cold-acclimated for 1 d), or 0.6 M (cold-acclimated for 7 d) sorbitol solution containing 1 mM MES/KOH, pH 5.6, and either 1 mM $CaCl_2$ or 1 mM EGTA. Freezing tolerance tests with protoplasts were performed according to a method previously described (Uemura et al., 1995). For the mechanical stress tolerance test, 200 μL of protoplast suspension was placed in a 4-mm cuvette and then subjected to electroporation using a square-wave pulse for 2 ms at 100 V (Gene Pulser; Bio-Rad). To simulate osmotic stress caused by freeze-induced dehydration, protoplast suspensions were added into a 4 M sorbitol solution (final concentration, 2.15 M) containing 1 mM MES/KOH, pH 5.6, and either 1 mM $CaCl_2$ or 1 mM EGTA at 0°C. Subsequently, an aliquot of no-sorbitol solution was added to the suspension to obtain an isotonic condition (0.6 M). Survival of protoplasts was determined using 0.001% (w/v) fluorescein diacetate (Wako) as previously described (Uemura et al., 1995).

Cryomicroscopy and Image Analyses

Fluorescence changes in cells during freeze/thawing were monitored using a cryomicroscope consisting of an upright fluorescence microscope with a 100-W mercury lamp (BX61; Olympus) and a cryostage (THMS600; Linkam). The cryostage possesses a silver block on which the temperature is controlled with liquid nitrogen and a built-in heating system. The temperature of the block was monitored by a platinum resistance temperature detector in the block (accuracy, <0.1°C). A filter set of U-MNIBA2 (Olympus) was used for the observation of BCECF fluorescence. Images obtained during the freeze/thawing process were recorded by a cooled CCD camera (CoolSNAP$_{HQ}$; Photometrics). For leaf sections, confocal images were obtained using a disk scanning unit system (BX-DSU; Olympus) and then deconvolved using the SlideBook ver. 4.1 program (Intelligent Imaging Innovations).

Test for the Survival of Leaf Sections

A test for the survival of leaf sections was performed with a fluorescent probe, BCECF acetoxymethyl ester (AM) (Molecular Probes), under a cryomicroscope. BCECF AM is not fluorescent but is membrane permeable, while BCECF is fluorescent but is not membrane permeable. After BCECF AM enters living cells and is cut by esterase, fluorescent BCECF is kept in living cells. Leaf sections 75 to 80 μm in thickness were prepared from *Arabidopsis* plants that were cold-acclimated for 7 d using a microtome with a vibrating blade (HM 650 V; MICROM International) in a buffer containing 1 mM MES/KOH, pH 5.6. Leaf sections were then stained with 0.001% (w/v) BCECF AM for 5 min at room temperature and subsequently washed to remove free BCECF AM. After being placed in a 0 or 0.6 M sorbitol solution containing 1 mM MES/KOH, pH 5.6, in the presence of either 1 mM $CaCl_2$ or 1 mM EGTA, leaf sections were transferred to a cover glass, which was surrounded by a 100-μm spacer and silicon grease. The sample was placed on the block of the cryostage. In the 0.6 M sorbitol condition, leaf sections were cooled to –2°C from 0°C at 0.5°C/min, during which ice nucleation started. After an additional 30-min incubation at –2°C, the sample was cooled to –12°C at 0.05°C/min and then thawed to 0°C at 1°C/min. In the case of 0 M sorbitol condition, leaf sections were cooled to –3°C from 0°C at 0.05°C/min and then thawed to 0°C at 1°C/min. The number of living cells was counted using an image analysis program, Image-Pro Plus ver. 5.1 (Media Cybernetics), and survival was calculated from the number of living cells before and after freeze/thawing.

Observation of Ice Distribution

Because fluorescent probes were found only in unfrozen solution sites, but not in ice crystals, the interface of ice crystals (that is, narrow lines of fluorescent unfrozen solution) is made visible by rejection of fluorescent probes from ice crystals, and consequently ice crystals can be negatively observed (Neils and Diller, 2004). Based on this concept, the ice distribution was observed with the cryomicroscope in a solution containing 1 mM Tris-HCl, pH 7.2, 1 mM $CaCl_2$, and 0.001% (w/v) BCECF (Molecular Probes), a plasma membrane–impermeable fluorescent probe.

Membrane Isolation and Immunochemical Analysis

A crude membrane fraction, prepared according to the method of Uemura et al. (1995), was suspended in a solution containing 5 mM MOPS/KOH, pH 7.3, 0.3 M sucrose, 1 mM EGTA, and 2 mM DTT and then layered onto a 36-mL linear gradient of 15 to 50% (w/w) sucrose in 5 mM MOPS/KOH, pH 7.3, 1 mM EGTA, and 2 mM DTT. After centrifugation at 28,000 rpm (141,000*g* Rmax) in a P28S swing rotor (Hitachi) for 20 h at 4°C, 0.5-mL fractions were collected. A highly purified plasma membrane fraction was isolated from *Arabidopsis* leaves according to a method described previously (Kawamura and Uemura, 2003). The antigen peptide and antibody were obtained from T.K. Craft (Japan). For polyclonal antibody preparation, the antigen peptide, which corresponds to the partial sequence of the C_2A-domain of SYT1 (VKHKNLNPEWNEEFKFSVRD), was linked with keyhole limpet hemocyanin as a carrier protein and then injected into rabbits. The immunoglobulin G fraction was prepared from the antiserum by affinity chromatography on a Protein G column (Amersham Biosciences). After neutralization, the immunoglobulin G fraction was desalted on a PD10 column (Amersham Biosciences) with MilliQ water, and the final protein concentration of the antibody was adjusted to 200 μg/mL (~1.3 μM). After the addition of antigen peptide (to a final concentration of 10 μM) into the antibody solution, the mixture of antibody and antigen peptide was kept at 0°C overnight. Polyacrylamide gel electrophoresis (12% [w/v]) and immunoblot analyses were performed according to standard procedures. The antigens on PVDF membranes were visualized using ECL (BD Healthcare).

Electrolyte Leakage Assay

Freezing injury of leaves was assayed by electrolyte leakage according to a previously published method (Uemura et al., 1995). Seeds of RNAi lines were planted on culture plates of Murashige and Skoog medium containing 0.8% (w/v) agar with or without 100 μg/mL BASTA. Ten-day-old plants were transferred to soil and then cultured in normal conditions for 4 weeks. Seeds of T-DNA mutants were directly sowed in soil. The 3rd to 5th leaves were used for electrolyte leakage tests.

Plant Freezing and Regrowth Assay

Plants of *SYT1*-RNAi lines and control *GFP*-RNAi lines were grown on Murashige and Skoog medium containing 0.8% (w/v) agar and 0.01% (w/v) BASTA in square dishes for 5 d, and then antibiotic-selected plants were transferred into new medium. Plants of the T-DNA insertion line and wild-type plants were grown in the above conditions without BASTA. Ten-day-old plants were cold-acclimated for 7 d. The samples were transferred into a programmable freezer (Espec) at −10°C, kept at the same temperature for 12 h, and then thawed at 2°C for 6 h. After thawing, the samples were grown for 10 d in the light and temperature conditions described above before their photographs were taken.

Statistical Analysis

All statistical analyses were performed with Mathematica ver. 6.0 (Wolfram Research).

Accession Numbers

Sequence data from this article can be found in the Arabidopsis Genome Initiative or GenBank/EMBL databases under the following accession numbers: SYT1 (At2g20990), RAFL05-21-F01; SYT2 (At1g20080); SYT3 (At5g04220), AY059741 and BX830716; SYT4 (At5g11100); SYT5 (At1g05500); ACTIN2 (At3g18780); RD29A (At5g52310); GUS, EG11055; GFP, EF090408; SALK T-DNA insertion mutants of SYT1, SAIL_775_A08

Supplemental Data

The following materials are available in the online version of this article.

Supplemental Figure 1. Ice Distribution Patterns in Leaf Sections of Wild-Type Plants.

Supplemental Figure 2. Identification of a Line with a T-DNA Insertion at the *SYT1* Locus.

Supplemental Figure 3. Extracellular Calcium-Dependent Tolerance to Mechanical Stress in RNAi Lines.

Supplemental Figure 4. Expression of *SYT* Genes, and Cold-Inducible *COR15a* and *RD29A* Genes.

ACKNOWLEDGMENTS

This study was supported by a grant from the 21st Century Circle of Excellence Program to Iwate University (K-03), Grants-in-Aid for Scientific Research (18780242 to Y.K., 20780229 to T.Y., and 17380062 to M.U.) from the Ministry of Education, Culture, Sports, Science, and Technology of Japan, and the President Fund of Iwate University. We thank M. Maeshima (Nagoya University, Japan) for kindly providing the antibodies of plasma membrane aquaporin and N. Masuko and M. Watanabe in our laboratory for their technical assistance.

Received September 24, 2008; revised October 31, 2008; accepted November 30, 2008; published December 16, 2008.

REFERENCES

Aguilar, P.S., Engel, A., and Walter, P. (2007). The plasma membrane proteins Prm1 and Fig1 ascertain fidelity of membrane fusion during yeast mating. Mol. Biol. Cell **18:** 547–556.

Bai, J., and Chapman, E.R. (2004). The C2 domains of synaptotagmin – Partners in exocytosis. Trends Biochem. Sci. **29:** 143–151.

Bansal, D., Miyake, K., Vogel, S.S., Groh, S., Chen, C.C., Williamson, R., McNeil, P.L., and Campbell, K.P. (2003). Defective membrane repair in dysferlin-deficient muscular dystrophy. Nature **423:** 168–172.

Bi, G.Q., Alderton, J.M., and Steinhardt, R.A. (1995). Calcium-regulated exocytosis is required for cell membrane resealing. J. Cell Biol. **131:** 1747–1758.

Chakrabarti, S., Kobayashi, K.S., Flavell, R.A., Marks, C.B., Miyake, K., Liston, D.R., Fowler, K.T., Gorelick, F.S., and Andrews, N.W. (2003). Impaired membrane resealing and autoimmune myositis in synaptotagmin VII-deficient mice. J. Cell Biol. **16:** 543–549.

Chang, D.C., and Reese, T.S. (1990). Changes in membrane structure induced by electroporation as revealed by rapid-freezing electron microscopy. Biophys. J. **58:** 1–12.

Craxton, M. (2004). Synaptotagmin gene content of the sequenced genomes. BMC Genomics **5:** 43.

Ezaki, N., Kido, N., Takahashi, K., and Katou, K. (2005). The role of

wall Ca^{2+} in the regulation of wall extensibility during the acid-induced extension of soybean hypocotyl cell walls. Plant Cell Physiol. **46:** 1831–1838.

Freeman, S.A., Wang, M.A., and Weaver, J.C. (1994). Theory of electroporation of planar bilayer membranes: predictions of the aqueous area, change in capacitance, and pore-pore separation. Biophys. J. **67:** 42–56.

Fujikawa, S., Kuroda, K., Jitsuyama, Y., Sano, Y., and Ohtani, J. (1999). Freezing behavior of xylem ray parenchyma cells in softwood species with differences in the organization of cell walls. Protoplasma **206:** 31–40.

Fujikawa, S., and Takabe, K. (1996). Formation of multiplex lamellae by equilibrium slow freezing of cortical parenchyma cells of mulberry and its possible relationship to freezing tolerance. Protoplasma **190:** 189–203.

Fukuda, M., Kanno, E., Satoh, M., Saegusa, C., and Yamamoto, A. (2004). Synaptotagmin VII is targeted to dense-core vesicles and regulates their Ca^{2+}-dependent exocytosis in PC12 cells. J. Biol. Chem. **279:** 52677–52684.

Griffith, M., Lumb, C., Wiseman, S.B., Wisniewski, M., Johnson, R. W., and Marangoni, A.G. (2005). Antifreeze proteins modify the freezing process in planta. Plant Physiol. **138:** 330–340.

Hepler, P.K., and Wayne, R.O. (1985). Calcium and plant development. Annu. Rev. Plant Physiol. **36:** 397–439.

Huynh, C., Roth, D., Ward, D.M., Kaplan, J., and Andrews, N.W. (2004). Defective lysosomal exocytosis and plasma membrane repair in Chediak-Higashi/beige cells. Proc. Natl. Acad. Sci. USA **101:** 16795–16800.

Ide, H., Price, W.S., Arata, Y., and Ishikawa, M. (1998). Freezing behaviors in leaf buds of cold-hardy conifers visualized by NMR microscopy. Tree Physiol. **18:** 451–458.

Ishikawa, M., Price, W.S., Ide, H., and Arata, Y. (1997). Visualization of freezing behaviors in leaf and flower buds of full-noon maple by nuclear magnetic resonance microscopy. Plant Physiol. **115:** 1515–1524.

Jackson, M.B., and Chapman, E.R. (2006). Fusion pores and fusion machines in Ca^{2+}-triggered exocytosis. Annu. Rev. Biophys. Biomol. Struct. **35:** 135–160.

Kawamura, Y., and Uemura, M. (2003). Mass spectrometric approach for identifying putative plasma membrane proteins of *Arabidopsis* leaves associated with cold acclimation. Plant J. **36:** 141–154.

Levitt, J. (1980). Responses of Plants to Environmental Stresses. (New York: Academic Press).

Los, D.A., and Murata, N. (2004). Membrane fluidity and its roles in the perception of environmental signals. Biochim. Biophys. Acta **1666:** 142–157.

Lynch, D.V., and Steponkus, P.L. (1987). Plasma membrane lipid alterations associated with cold acclimation of winter rye seedlings (*Secale cereale* L. cv Puma). Plant Physiol. **83:** 761–767.

Lynch, K.L., Gerona, R.R., Larsen, E.C., Marcia, R.F., Mitchell, J.C., and Martin, T.F. (2007). Synaptotagmin C_2A loop 2 mediates Ca^{2+}-dependent SNARE interactions essential for Ca^{2+}-triggered vesicle exocytosis. Mol. Biol. Cell **18:** 4957–4968.

McNeil, A.K., Rescher, U., Gerke, V., and McNeil, P.L. (2006). Requirement for annexin A1 in plasma membrane repair. J. Biol. Chem. **281:** 35202–35207.

McNeil, P.L., and Kirchhausen, T. (2005). An emergency response team for membrane repair. Nat. Rev. Mol. Cell Biol. **6:** 499–505.

Mellgren, R.L., Zhang, W., Miyake, K., and McNeil, P.L. (2007). Calpain is required for the rapid, calcium-dependent repair of wounded plasma membrane. J. Biol. Chem. **282:** 2567–2575.

Mills, L.R., and Morris, C.E. (1998). Neuronal plasma membrane dynamics evoked by osmomechanical perturbations. J. Membr. Biol. **166:** 223–235.

Morris, C.E., and Homann, U. (2001). Cell surface area regulation and membrane tension. J. Membr. Biol. **179:** 79–102.

Murai, M., and Yoshida, S. (1998). Evidence for the cell wall involvement in temporal changes in freezing tolerance of Jerusalem artichoke (*Helianthus tuberosus* L.) tubers during cold acclimation. Plant Cell Physiol. **39:** 97–105.

Neils, C.M., and Diller, K.R. (2004). An optical-axis freezing stage for laser-scanning microscopy of broad ice-water interfaces. J. Microsc. **216:** 249–262.

Nicot, N., Hausman, J.F., Hoffmann, L., and Evers, D. (2005). Housekeeping gene selection for real-time RT-PCR normalization in potato during biotic and abiotic stress. J. Exp. Bot. **56:** 2907–2914.

Niwa, Y., Hirano, T., Yoshimoto, K., Shimizu, M., and Kobayashi, H. (1999). Non-invasive quantitative detection and applications of non-toxic, S65T-type green fluorescent protein in living plants. Plant J. **18:** 455–463.

Ohshima, Y., Iwasaki, I., Suga, S., Murakami, M., Inoue, K., and Maeshima, M. (2001). Low aquaporin content and low osmotic water permeability of the plasma and vacuolar membranes of a CAM plant *Graptopetalum paraguayense*: Comparison with radish. Plant Cell Physiol. **42:** 1119–1129.

Olien, C.R. (1974). Energies of freezing and frost desiccation. Plant Physiol. **53:** 764–767.

Olien, C.R., and Smith, M.N. (1977). Ice adhesions in relation to freeze stress. Plant Physiol. **60:** 499–503.

Palmgren, M.G., Askerlund, P., Fredrikson, K., Widell, S., Sommarin, M., and Larsson, C. (1990). Sealed inside-out and right-side-out plasma membrane vesicles: Optimal conditions for formation and separation. Plant Physiol. **92:** 871–880.

Pearce, R.S. (1988). Extracellular ice and cell shape in frost-stressed cereal leaves: A low-temperature scanning-electron-microscopy study. Planta **175:** 313–324.

Pearce, R.S., and Ashworth, E.N. (1992). Cell shape and localisation of ice in leaves of overwintering wheat during frost stress in the field. Planta **188:** 324–331.

Puhakainen, T., Hess, M.W., Makela, P., Svensson, J., Heino, P., and Palva, E.T. (2004). Overexpression of multiple dehydrin genes enhances tolerance to freezing stress in Arabidopsis. Plant Mol. Biol. **54:** 743–753.

Raucher, D., and Sheetz, M.P. (1999). Characteristics of a membrane reservoir buffering membrane tension. Biophys. J. **77:** 1992–2002.

Reddy, A., Caler, E.V., and Andrews, N.W. (2001). Plasma membrane repair is mediated by Ca^{2+}-regulated exocytosis of lysosomes. Cell **106:** 157–169.

Reyes-Diaz, M., Ulloa, N., Zuniga-Feest, A., Gutierrez, A., Gidekel, M., Alberdi, M., Corcuera, L.J., and Bravo, L.A. (2006). *Arabidopsis thaliana* avoids freezing by supercooling. J. Exp. Bot. **57:** 3687–3696.

Ristic, Z., and Ashworth, E.N. (1993). Changes in leaf ultrastructure and carbohydrates in *Arabidopsis thaliana* L. (Heyn) cv. Columbia during rapid cold acclimation. Protoplasma **172:** 111–123.

Schapire, A.L., Voigt, B., Jasik, J., Rosado, A., Lopez-Cobollo, R., Menzel, D., Salinas, J., Mancuso, S., Valpuesta, V., Baluska, F., and Botella, M.A. (2008). *Arabidopsis* synaptotagmin 1 is required for the maintenance of plasma membrane integrity and cell viability. Plant Cell **20:** 3374–3388.

Schonn, J.S., Maximov, A., Lao, Y., Sudhof, T.C., and Sorensen, J.B. (2008). Synaptotagmin-1 and -7 are functionally overlapping Ca^{2+} sensors for exocytosis in adrenal chromaffin cells. Proc. Natl. Acad. Sci. USA **105:** 3998–4003.

Seki, M., Carninci, P., Nishiyama, Y., Hayashizaki, Y., and Shinozaki,

K. (1998). High-efficiency cloning of *Arabidopsis* full-length cDNA by biotinylated CAP trapper. Plant J. **15:** 707–720.

Seki, M., et al. (2002a). Monitoring the expression profiles of 7000 *Arabidopsis* genes under drought, cold and high-salinity stresses using a full-length cDNA microarray. Plant J. **31:** 279–292.

Seki, M., et al. (2002b). Functional annotation of a full-length *Arabidopsis* cDNA collection. Science **296:** 141–145.

Shen, S.S., Tucker, W.C., Chapman, E.R., and Steinhardt, R.A. (2005). Molecular regulation of membrane resealing in 3T3 fibroblasts. J. Biol. Chem. **280:** 1652–1660.

Solecka, D., Zebrowski, J., and Kacperska, A. (2008). Are pectins involved in cold acclimation and de-acclimation of winter oil-seed rape plants? Ann. Bot. (Lond.) **101:** 521–530.

Stein, A., Radhakrishnan, A., Riedel, D., Fasshauer, D., and Jahn, R. (2007). Synaptotagmin activates membrane fusion through a Ca^{2+}-dependent trans interaction with phospholipids. Nat. Struct. Mol. Biol. **14:** 904–911.

Steinhardt, R.A., Bi, G., and Alderton, J.M. (1994). Cell membrane resealing by a vesicular mechanism similar to neurotransmitter release. Science **263:** 390–393.

Steponkus, P.L., Uemura, M., and Webb, M.S. (1993). A contrast of the cryostability of the plasma membrane of winter rye and spring ort: Two species that widely differ in their freezing tolerance and plasma membrane lipid composition. In Advances in Low-Temperature Biology, P.L. Steponkus, ed (London: JAI Press), pp. 211–312.

Thomashow, M.F. (1999). Plant cold acclimation: Freezing tolerance genes and regulatory mechanisms. Annu. Rev. Plant Physiol. Plant Mol. Biol. **50:** 571–599.

Thorlby, G., Fourrier, N., and Warren, G. (2004). The *SENSITIVE TO FREEZING2* gene, required for freezing tolerance in *Arabidopsis thaliana*, encodes a beta-glucosidase. Plant Cell **16:** 2192–2203.

Towill, L.E., and Mazur, P. (1976). Osmotic shrinkage as a factor in freezing injury in plant tissue cultures. Plant Physiol. **57:** 290–296.

Uemura, M., Joseph, R.A., and Steponkus, P.L. (1995). Cold acclimation of *Arabidopsis thaliana*: Effect on plasma membrane lipid composition and freeze-induced lesions. Plant Physiol. **109:** 15–30.

Uemura, M., and Steponkus, P.L. (1994). A contrast of the plasma membrane lipid composition of oat and rye leaves in relation to freezing tolerance. Plant Physiol. **104:** 479–496.

Uemura, M., Tominaga, Y., Nakagawara, C., Shigematsu, S., Minami, A., and Kawamura, Y. (2006). Responses of the plasma membrane to low temperatures. Physiol. Plant. **126:** 81–89.

Uemura, M., and Yoshida, S. (1984). Involvement of plasma membrane alterations in cold acclimation of winter rye seedlings (*Secale cereale* L. cv Puma). Plant Physiol. **75:** 818–826.

Uemura, M., and Yoshida, S. (1986). Studies on freezing injury in plant cells. II. Protein and lipid changes in the plasma membranes of Jerusalem artichoke tubers during a lethal freezing in vivo. Plant Physiol. **80:** 187–195.

Yamaguchi-Shinozaki, K., and Shinozaki, K. (1994). A novel *cis*-acting element in an *Arabidopsis* gene is involved in responsiveness to drought, low-temperature, or high-salt stress. Plant Cell **6:** 251–264.

Yamazaki, T., Kawamura, Y., and Uemura, M. (2008). Cryobehavior of the plasma membrane in protoplasts isolated from cold-acclimated *Arabidopsis* leaves is related to surface area regulation. Plant Cell Physiol. **49:** 944–957.

Yoshida, S. (1984). Chemical and biophysical changes in the plasma membrane during cold acclimation of mulberry bark cells (*Morus bombycis* Koidz. cv Goroji). Plant Physiol. **76:** 257–265.

Yoshida, S., and Uemura, M. (1984). Protein and lipid compositions of isolated plasma membranes from orchard grass (*Dactylis glomerata* L.) and changes during cold acclimation. Plant Physiol. **75:** 31–37.